Pansharpening by A Nonlocal Channel-Decoupled Variational Method

Joan Duran†, Antoni Buades†, Bartomeu Coll†, Catalina Sbert†, and Gwendoline Blanchet‡

†Department of Mathematics and Computer Science, University of Balearic Islands, Spain

‡Centre National d'Études Spatiales, Toulouse, France

Abstract

We propose a variational model for which pansharpening is defined as an optimization problem minimizing a cost function with nonlocal regularization. We incorporate a new term preserving the radiometric ratio between the panchromatic and each spectral band. The resulting model is channel-decoupled, thus permitting the application to misregistered spectral data. The experimental results illustrate the superiority of the proposed method with respect to the state of the art to preserve spatial details, reduce color artifacts, and avoid aliasing.

1. Introduction

Many Earth observation satellites decouple the acquisition of a panchromatic image at high spatial resolution from the acquisition of a multispectral image at lower spatial resolution. Pansharpening is the fusion process by which a high-resolution multispectral image is inferred.

Panchromatic — *Red, green, blue, near-infrared* — *Low-resolution multispectral*

Pansharpening has been an intensive field of research [1]. Most of state-of-the-art methods need all data to be geometrically aligned. Unfortunately, this is not satisfied by satellite imagery, for which different spectral bands are not co-registered and their registration previously to pansharpening is not recommendable due to strong aliasing.

We propose a nonlocal variational model for pansharpening. Compared to [2], the classical assumption on the linear dependence of the panchromatic and spectral components is replaced by a radiometric constraint. The minimization can be performed independently for each band, thus permitting the application to misregistered spectral data.

2. Variational Formulation of Pansharpening

Let $\Omega \subset \mathbb{R}^M$ be an open and bounded domain and C, the number of spectral bands. The satellite data consist of

- a high-resolution panchromatic image $P : \Omega \to \mathbb{R}$,
- a low-resolution multispectral image $\mathbf{u}^S : S \to \mathbb{R}^C$ defined on a sampling grid $S \subseteq \Omega$.

The high-resolution multispectral image to be inferred is denoted by $\mathbf{u} : \Omega \to \mathbb{R}^C$.

Inverse Problem. The most common image formation model, pioneered by Ballester *et al* [3], assumes that

$$u_k^S = (\kappa_k * u_k)^{\downarrow_s} + \eta_k, \quad \forall k \in \{1, \dots, C\}, \tag{1}$$

where $\downarrow_s$ denotes the subsampling operator by a factor s (for most satellites, $s = 4$), κ_k is the impulse response for the kth spectral band, and η_k is i.i.d. zero-mean Gaussian noise.

Panchro-Spectral Constraint. Ballester *et al* [3] further incorporated the following constraint:

$$P(\mathbf{x}) = \sum_{k=1}^{C} \alpha_k u_k(\mathbf{x}), \quad \forall \mathbf{x} \in \Omega,$$

where $\{\alpha_k\}$ are mixing coefficients. Importantly, it is assumed here that all spectral bands are co-registered.

Classical Regularization Strategies. Ballester *et al* [3] proposed to regularize the solution of (1) by aligning all level lines of P and each u_k. Several variants of the total variation regularization have been also used so far [1].

Nonlocal Regularization. Nonlocal methods use a similarity measure relating points in the whole domain having similar geometry and texture. In [2], we introduced nonlocal regularization into pansharpening through the energy

$$\int_\Omega \int_\Omega (u_k(\mathbf{y}) - u_k(\mathbf{x}))^2 \, \omega_P(\mathbf{x}, \mathbf{y}) \, d\mathbf{y} \, d\mathbf{x}, \tag{2}$$

where the similarity distribution $\omega_P : \Omega \times \Omega \to \mathbb{R}$ is

$$\omega_P(\mathbf{x}, \mathbf{y}) = \frac{1}{\Upsilon(\mathbf{x})} \exp\left(-\frac{d\left(P(\mathbf{x}), P(\mathbf{y})\right)}{h^2}\right). \tag{3}$$

$\Upsilon(\mathbf{x})$ is a normalization factor and $d(P(\mathbf{x}), P(\mathbf{y}))$ computes the distance between neighborhoods around $\mathbf{x}$ and $\mathbf{y}$.

3. Nonlocal Channel-Decoupled Model

Radiometric Constraint. Let P_k be the panchromatic in the reference of u_k and $P_k^S : S \to \mathbb{R}$, its decimation as in (1). Let $\widetilde{P}_k : \Omega \to \mathbb{R}$ and $\widetilde{u}_k : \Omega \to \mathbb{R}$ be the extensions of P_k^S and u_k^S to Ω by interpolation. We encourage that

$$\frac{u_k(\mathbf{x})}{P_k(\mathbf{x})} = \frac{\widetilde{u}_k(\mathbf{x})}{\widetilde{P}_k(\mathbf{x})}, \quad \forall \mathbf{x} \in \Omega, \quad \forall k \in \{1, \dots, C\}, \tag{4}$$

which is equivalent to

$$u_k(\mathbf{x}) - \widetilde{u}_k(\mathbf{x}) = \frac{\widetilde{u}_k(\mathbf{x})}{\widetilde{P}_k(\mathbf{x})} \left(P_k(\mathbf{x}) - \widetilde{P}_k(\mathbf{x})\right), \quad \forall \mathbf{x} \in \Omega, \quad \forall k \in \{1, \dots, C\}.$$

Thus, we force the high frequencies of each spectral band to coincide with those of the panchromatic. Importantly, we require each P_k to be registered with the kth channel, but nothing about the co-registration of spectral data.

The Energy Functional. We propose the following channel-decoupled energy functional:

$$J_2(\mathbf{u}) = \sum_{k=1}^{C} J_2(u_k) \tag{5a}$$

such that

$$J_2(u_k) = \frac{1}{2} \int_\Omega \int_\Omega (u_k(\mathbf{y}) - u_k(\mathbf{x}))^2 \omega_{P_k}(\mathbf{x}, \mathbf{y}) \, d\mathbf{y} \, d\mathbf{x} + \frac{\mu s^2}{2} \int_\Omega \Pi_S \cdot \left(\kappa_k * u_k(\mathbf{x}) - u_k^\Omega(\mathbf{x})\right)^2 d\mathbf{x} + \frac{\delta}{2\|P_k\|^2} \int_\Omega \left(u_k(\mathbf{x}) \widetilde{P}_k(\mathbf{x}) - \widetilde{u}_k(\mathbf{x}) P_k(\mathbf{x})\right)^2 d\mathbf{x}. \tag{5b}$$

- The first term corresponds to the nonlocal regularization (2) with the weights ω_{P_k} defined in (3).
- The second term is the variational formulation of (1), where $\Pi_S = \sum_{\mathbf{x} \in S} \delta_{\mathbf{x}}$ is a Dirac's comb defined by the sampling grid S and $\mathbf{u}^\Omega : \Omega \to \mathbb{R}^C$ is an arbitrary extension of $\mathbf{u}^S$ as a continuous function from S to Ω.
- The third term is the Lagrangian formulation associated to the radiometric constraint (4).

Using standard arguments from convex analysis, we prove that the minimization of (5) admits an unique solution.

Numerical minimization. Using the gradient descent method, the solution is obtained by iterating the equation

$$u_k^{(n+1)}(\mathbf{p}) = u_k^{(n)}(\mathbf{p}) - \tau \sum_{\mathbf{q} \in I} \left(u_k^{(n)}(\mathbf{p}) - u_k^{(n)}(\mathbf{q})\right) \left(\omega_{P_k}(\mathbf{p}, \mathbf{q}) + \omega_{P_k}(\mathbf{q}, \mathbf{p})\right) - \tau \mu s^2 \left(K_k^\top \Pi_S \left(K_k u_k^{(n)} - u_k^\Omega\right)\right)(\mathbf{p}) - \tau \frac{\delta}{\|P_k\|^2} \left(u_k^{(n)}(\mathbf{p}) \widetilde{P}_k(\mathbf{p}) - \widetilde{u}_k(\mathbf{p}) P_k(\mathbf{p})\right) \widetilde{P}_k(\mathbf{p}), \tag{6}$$

where $n \geq 0$ is the iteration number and τ is the artificial time step in the descent direction. Here, K_k is the blurring matrix associated to κ_k and Π_S is implemented by taking every fourth pixel to be one along each direction. For computational purposes, the nonlocal term is limited to interact between pixels at a distance given by $\nu_r > 0$, i.e.

$$\omega_{P_k}(\mathbf{p}, \mathbf{q}) = \begin{cases} \frac{1}{\Upsilon(\mathbf{p})} \exp\left(-\frac{1}{h^2} \sum_{\{\mathbf{t} : \|\mathbf{t}\|_\infty \leq \nu_c\}} |P_k(\mathbf{p} + \mathbf{t}) - P_k(\mathbf{q} + \mathbf{t})|^2\right) & \text{if } \|\mathbf{p} - \mathbf{q}\|_\infty \leq \nu_r, \\ 0 & \text{otherwise,} \end{cases}$$

where $\nu_c > 0$ determines the size of a window centered at $\mathbf{0}$ and $\Upsilon(\mathbf{p})$ is the normalization factor. To avoid an excessive weighting of the reference pixel, $\omega_{P_k}(\mathbf{p}, \mathbf{p})$ is set to the maximum of the weights.

Proposed Algorithm. Since (6) decouples for each spectral component, we can proceed as follows:

i) Superimpose the panchromatic image, which hardly contains aliasing, on the reference of u_k.
ii) Compute the weight function ω_{P_k} on the registered panchromatic.
iii) Solve the pansharpening problem for u_k by iterating (6) until convergence.
iv) Superimpose all high-resolution spectral bands on a common geometry for visualization purposes.

We avoid resampling the aliased spectral components and the algorithm applies on the original data instead.

4. Experimental Results

- We compare the performance of the proposed model with some of the best state-of-the-art pansharpening techniques according to [1].
- Data simulated from full-color aerial images at 30 cm: panchromatic obtained by averaging the reference color channels; low-resolution multispectral components obtained by translating the reference color channels and then filtering them with Gaussian kernel of standard deviation 1.7 followed by subsampling of factor $s = 4$.
- All techniques except ATWT, GLP, and ours require co-registered spectral components.

Methods	RMSE	SAM	SSIM
Reference	0	0	1
Co-registered spectral data			
Brovey [4]	2.7954	1.7668	0.9937
BDSD [5]	1.9628	2.0636	0.9979
PRACS [6]	2.3621	1.5384	0.9976
ATWT [7]	2.2277	1.5484	0.9980
AWLP [8]	2.0889	1.4481	0.9982
GLP [9]	2.0919	1.3451	0.9980
P+XS [3]	1.9259	1.7746	0.9985
NLV [2]	1.6488	1.3790	0.9987
Ours	1.7785	1.5380	0.9984
Misregistered spectral data			
ATWT [7]	2.1991	1.5669	0.9983
GLP [9]	2.2191	1.5535	0.9980
Ours	**1.2539**	**0.9379**	**0.9997**

Average of each metric over the dataset. RMSE accounts for spatial distortion, SAM measures the spectral distortion, and SSIM measures loss of correlation, luminance, and contrast distortion

Dataset of full-color aerial images

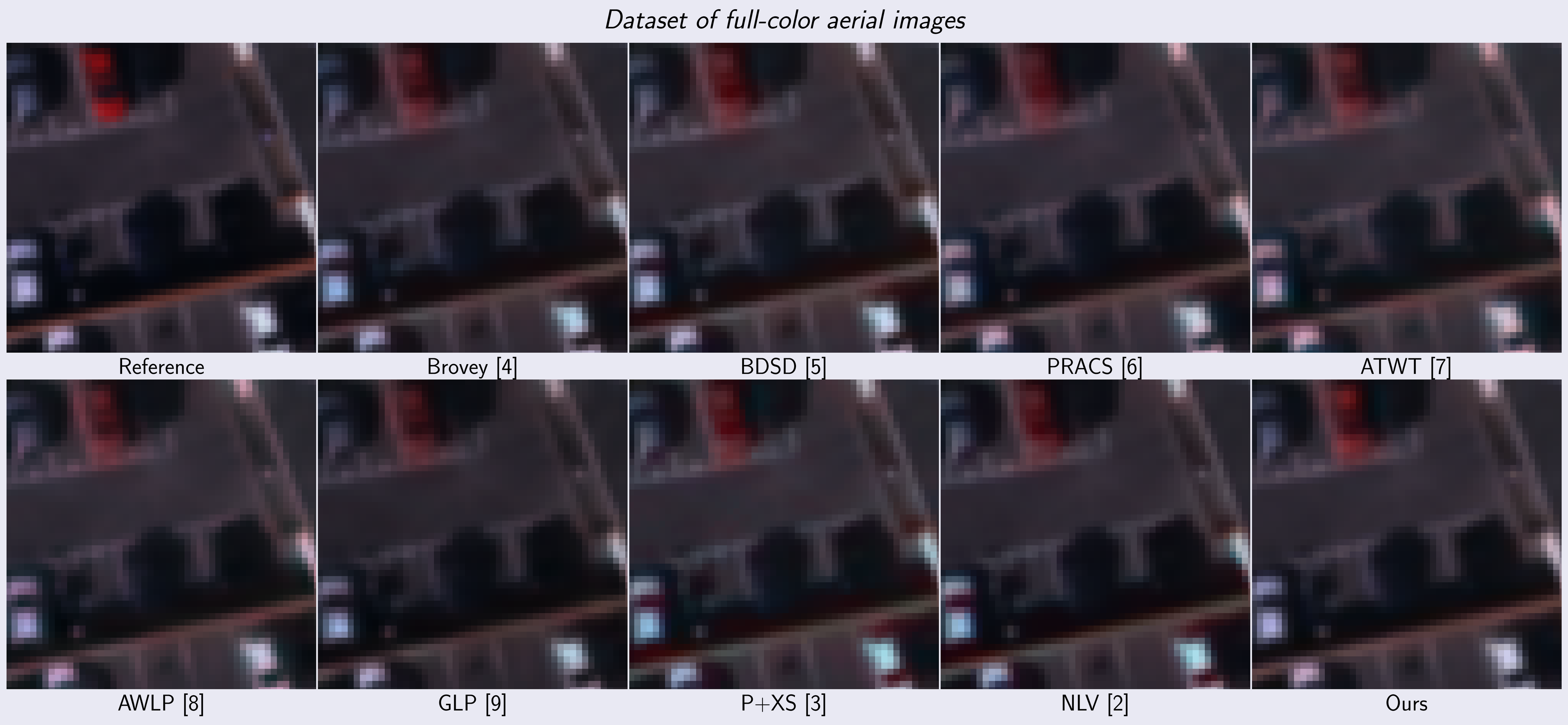

All results except ours are affected by aliasing, e.g. see the alias pattern along the light brown wall. The spots on the white cars, the reduction of the chromatic saturation, and the colors of the objects exceeding their contours also compromise the performances of all the other methods

5. Conclusions

- We have introduced a nonlocal channel-decoupled variational model for pansharpening.
- The method does not need the spectral data to be co-registered and suppresses any assumption on the linear dependence of the panchromatic and spectral modalities.
- The proposed method performs the best on simulated data compared to state-of-the-art techniques.

References

[1] G. Vivone, L. Alparone, J. Chanussot, M. Dalla Mura, A. Garzelli, R. Restaino, G. Licciardi, and L. Wald, "A critical comparison among pansharpening algorithms," *IEEE Trans. Geosci. Remote Sens.*, vol. 53, no. 5, pp. 2565–2586, 2015.

[2] J. Duran, A. Buades, B. Coll, and C. Sbert, "A nonlocal variational model for pansharpening image fusion," *SIAM J. Imaging Sci.*, vol. 7, no. 2, pp. 761–796, 2014.

[3] C. Ballester, V. Caselles, L. Igual, J. Verdera, and B. Rougé, "A variational model for P+XS image fusion," *Int. J. Comput. Vis.*, vol. 69, no. 1, pp. 43–58, 2006.

[4] A.R. Gillespie, A.B. Kahle, and R.E. Walker, "Color enhancement of highly correlated images. II. Channel ratio and "chromacity" transform techniques," *Remote Sens. Environ.*, vol. 22, no. 3, pp. 343–365, 1987.

[5] A. Garzelli, F. Nencini, and L. Capobianco, "Optimal MMSE pan-sharpening of very high resolution multispectral images," *IEEE Trans. Geosci. Remote Sens.*, vol. 46, no. 1, pp. 228–236, 2008.

[6] J. Choi, K. Yu, and Y. Kim, "A new adaptive component-substitution based satellite image fusion by using partial replacement," *IEEE Trans. Geosci. Remote Sens.*, vol. 49, no. 1, pp. 295–309, 2011.

[7] G. Vivone, R. Restaino, M. Mura, G. Licciardi, and J. Chanussot, "Contrast and error-based fusion schemes for multispectral image pansharpening," *IEEE Geosci. Remote Sens. Lett.*, vol. 11, no. 5, pp. 930–934, 2014.

[8] X. Otazu, M. González-Audícana, O. Fors, and J. Nuñez, "Introduction of sensor spectral response into image fusion methods. Application to wavelet-based methods," *IEEE Trans. Geosci. Remote Sens.*, vol. 43, no. 10, pp. 2376–2385, 2005.

[9] B. Aiazzi, L. Alparone, S. Baronti, A. Garzelli, and M. Selva, "MTF-tailored multiscale fusion of high-resolution MS and Pan imagery," *Photogramm. Eng. Remote Sens.*, vol. 72, no. 5, pp. 591–596, 2006.

Acknowledgements

This work has been partially financed by CNES through the project R-S13/OT-0001-098. J. Duran, A. Buades, B Coll, and C. Sbert were also supported by the Ministerio de Ciencia e Innovación under grant TIN2014-53772-R.